Anatomy, functional anatomy and morphometrical study of forelimb column in Asiatic cheetah (Acinonyx jubatus venaticus)

Moahammad Naser Nazem*, Sayed Mohsen Sajjadian, Alireza Nakhaei

Department of Basic Sciences, School of Veterinary Medicine, Shahid Bahonar University of Kerman, Kerman, Iran

Abstract

The Asiatic cheetah (Acinonyx jubatus venaticus) is one of the most endangered members of the family Felidae in the world. However, there isn't enough information about anatomy and functional anatomy of its bones and muscles. The aim of this study was to investigate the anatomy, morphometry and function of forelimb column (humerus, radius, ulna).
The carrions of five adult Asiatic cheetahs were collected from the desert. Column bones of forelimbs were studied anatomically and relationship between their angles, tubers and origin and insertion of some important muscles in the Felidae were evaluated. Also some important parameters were measured. Results showed that very important characters of this animal were referred to their articular surfaces and tubers of their bones. Also the length and diameter of column bones and angles between origin and insertion of their muscles, especially brachioradialis muscle, play a high role in their anatomical function.

Key words

Asiatic cheetah, osteomorphometry, humerus, radius, ulna.

Introduction

The cheetah (*Acinonyx jubatus*) is probably best known for being the fastest land animal in the world with an estimated top speed of circa 112 km/h (Sunquist and Sunquist, 2002). Contrary to a widespread misconception that the cheetah "is not a cat", it is a full-fledged felid, most closely related to the puma (*Puma concolor*) and the jaguarundi (*P. yaguarondi*) (O'Brien and Johnson, 2007). The cheetah is roughly the same size as a leopard (*Panthera pardus*) – with which it is often confused – but is of a lighter and more slender build, has a smaller head, smaller teeth, and is a poor climber. The cheetah is also distinguished by dark tear-marks in the facial fur running down its eyes, towards the muzzle. Sexual dimorphism is not very pronounced in the cheetah (Hunter and Hamman, 2003).

The Asiatic cheetah (*Acinonyx jubatus venaticus*) is now one of the most endangered members of the family Felidae in the world. Over the past 20 years, Iran has been the last stronghold for the Asiatic cheetah, known in Iran as yuz, although there have been occasional reports of cheetahs across the border in Pakistan (Farhadinia,

2004). Today the Iranian cheetah (Asiatic cheetah) is one of the most endangered felids in the world (Farhadinia, 2004).

As mentioned the cheetah is widely acknowledged to be the fastest living land mammal and yet there is little scientific evidence to explain how it achieves such remarkable speeds (Hudson et al., 2011). To maximize its speed, an animal must rapidly swing its limbs (to increase stride frequency) and support its body weight by resisting large ground reaction forces (GRF) (Weyand et al., 2000). As a predator, the cheetah also uses its forelimbs for prey capture and therefore they must also be adapted for this function (Hudson et al., 2011).

Muscle fiber type composition will also play a large role in determining a muscle contraction velocity. Cheetah muscle has been shown to contain a high proportion of fast-twitch fibers (Williams et al., 1997), which would be highly beneficial for rapidly swinging the limb and reducing swing time; however, exact contraction velocities are unknown (Hudson et al., 2011).

With increasing speed, an animal stance time (Cavagna et al., 1988; Heglund and Taylor, 1988) and duty factor (proportion of a stride in which the feet are in contact with the ground; (Keller et al., 1996; Weyand et al., 2000) decrease. During the period of a stride in which the feet are in contact with the ground, an animal must support its body weight by resisting the GRF joint torques experienced by the limb (Alexander, 1985; Weyand et al., 2000; Usherwood and Wilson, 2006).

There have been some macro-anatomical investigations on the skeletal systems of large animals such as horse and cattle, small ruminants such as sheep (Getty, 1975), carnivores such as dog (Evans and de Lahunta, 2013), wild carnivores such as the mink and from the order of Rodentia such as guinea pig and rat (Ozkan et al., 1997; Yilmaz S. 1998), and from the order Lagomorpha such as rabbit (Ozkan et al., 1997), but the skeletal systems of Asiatic cheetah have not been investigated in detail. The last physical evidence of the cheetah in India was of three shot in 1947 by the ruler (Farhadinia, 2004). So the aim of this study was to investigate the osteomorphometry and functional anatomy of the bony elements of the cheetah fore-column (the humerus and radio–ulna: Nickle et al., 1973) in detail. This may be an added contribution to knowledge in the area of osteomorphometry and offer a foundation for establishing a morphofunctional paradigm to understand the peculiar adaptation features of the species.

Material and methods

Total carrions of five adult Asiatic cheetahs of both sexes were collected during 2009 to 2014 from the desert.

Column bones of forelimbs (humerus, radius, ulna) were then selected from each of them. The remaining skin fascia was removed. The origin and insertion of various muscles were marked and then the muscles were removed from the bones. Then the bones were boiled in soap water for long time for the easy removal of muscle tendons and ligaments. Before boiling, each forelimb was wrapped separately with net to prevent the loss of small bones. After boiling, the remained muscles and tendons were removed and washed with tap water. The bones were washed with bleaching powder to remove the unpleasant smell and dried at sunlight for two days and finally kept at room temperature for gross anatomical study.

The column bones in forelimb were described anatomically. Obtained results were compared with those in the cat. The cat bones had been provided previously in anatomy hall.

In order to study total length, width or breadth of the humerus, radius and ulna, these bones were measured, based on previous studies (Von den Driesch, 1976; Simon, 1996), by a Vernier caliper (sensitivity: 0.01 mm, MG6001DC, General Tools and Instruments Company, New York, USA). For this purpose the following measures were taken: (a) in the humerus: greatest length along the long axis of the bone from the apex of the greater trochanter to the lowest edge of trochlea (GL), greatest length from caput (head) along the long axis to the lowest edge of trochlea (GLC), greatest breadth of the proximal end (BP), greatest breadth of the distal end (BD), smallest breadth of the diaphysis (SD); in the radius: greatest length taken along the long axis of the bone "in projection" (GL); greatest proximal width including the area to which muscles are attached and perpendicular to the sagittal groove (BP); minimum diameter of the shaft (SD); greatest breadth of the distal end (BD); in the ulna: greatest length (GL); depth across the processus anconaeus (DPA); smallest depth of the olecranon (SDO); greatest breadth cross the coronoid process (BPC).

Results were expressed as mean ± standard error (SE). Data were analyzed by simple test, using the software SPSS 16 (Statistical Package for the Social Sciences, version 16, SPSS, Chicago, USA).

Results

A) Anatomical description

Humerus

The humerus was a long bone situated obliquely downward and backward; it formed the shoulder joint above with the scapula and elbow joint below with the radius and ulna.

The round articular head was at the proximal extremity on the caudomedial surface. It was strongly curved backwards proximo-distally. Under the head there was a narrow distinct neck. The greater tubercle was large, undivided and prominent on the cranial and lateral surface of the proximal bone extremity. This tuber showed a longer craniocaudal axis (Figs. 1 and 3). There was a round swelling on the cranial border of this tuber (Fig. 3).

The lesser tubercle was a short non articular, undivided prominence just under the head on the medial surface. The axis of this tuber was directed dorsoventrally and cranio-caudally. (Fig. 2). There was a wide bicipital groove between the two tubers on the craniomedial surface of the proximal extremity of this bone (Fig. 4).

The shaft was cylindrical and curved cranially (Fig. 1-3). The cross section of the proximal half of the diaphysis was oval with a craniocaudal long axis while it was rounded in the distal half (Figs 1, 3). This bone presented two surfaces, a lateral and a medial one. The lateral surface was spiral, smooth, and presented a shallow musculospiral groove which continued until the proximal half of this bone (Fig. 1, 3). The deltoid tuberosity was found less prominent at the margin between the lateral and medial surfaces (Fig. 4).
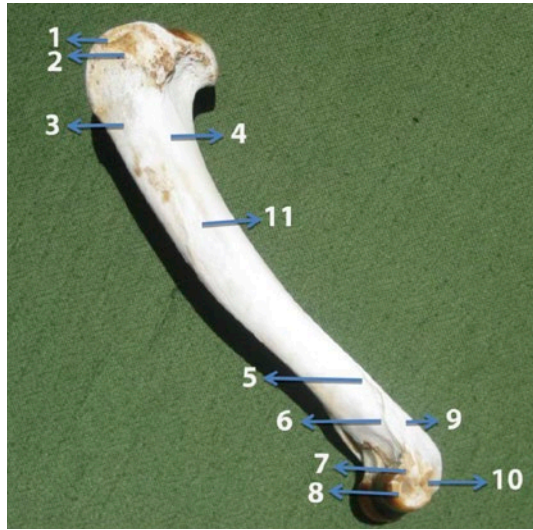
Figure 1. Craniolateral view of humerus: 1) Insertion of infraspinatus, 2) Teres minor tuberosity and insertion of teres minor, 3) Origin of brachialis, 4) Origin of lateral head of triceps, 5) Origin of extensor carpi radialis, 6) Origin of extensor digitorum communis, 7) Origin of extensor digitorum lateralis, 8) Origin of supinator, 9) Origin of anconeus, 10) Origin of extensor carpi ulnaris, 11) Musculospiral groove.

The radial and olecranon fossae of the humerus of the Asiatic cheetah were shallow (Figs. 5, 6). There was a slit-like supracondyloid foramen on the medial surface of the distal extremity immediately above the medial epicondyle. This oval foramen because of its position didn't connect the radial fossa with the olecranon fossa (Figs. 2, 6).

The epicondyloid crest of humerus was found prominent at the distolateral extremity of the diaphysis (Fig. 6). Two main nutrient foramens were observed on the shaft of this bone: one of them was on the roof of the olecranon fossa and the other one was situated on the medial surface, proximal to the supratrochlear foramen.

The distal extremity contained two condyles, lateral and medial, the latter was greater than the lateral one. Trochlea, the medial and larger part, was articulated with the ulna while capitulum, the lateral part, was articulated with the radius (Fig. 1, 6).

The smaller lateral epicondyle projected caudolaterally and the more prominent medial epicondyle caudomedially (Fig. 6). The two epicondyles were separated by olecranon fossa. Flanking the lateral condyle there were a shallow ligamentous depression and a large tubercle.

Radius and ulna

The radius and the ulna constituted the skeleton of the forearm or antebrachium which, in turn, made up the distal element of the bony column of the forelimb (Nickel et al., 1973). In the Asiatic cheetah there was a crossover between radius and ulna so that the proximal end of the ulna lied medially against the radius.
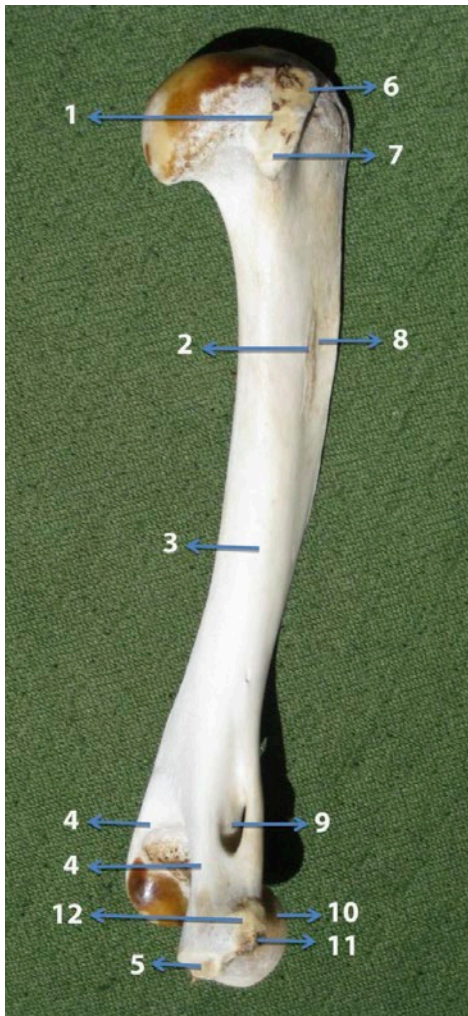
Figure 2. Caudomedial view of humerus: 1) Origin of accessory head of triceps, 2) Teres major tuberosity and insertion of teres major, 3) Origin of medial head of triceps, 4) Epicondyles of humerus and origin of anconeus, 5) Origin of humeral head of flexor carpi ulnaris, 6) Lesser tubercle and insertion of subscapularis, 7) Origin of coracobrachialis, 8) Insertion of latissimus dorsi, 9) Supracondyloid foramen, 10) Origin of pronator teres, 11) Origin of humeral head of deep digital flexor tendon, 12) Origin of super facial digital flexor tendon.
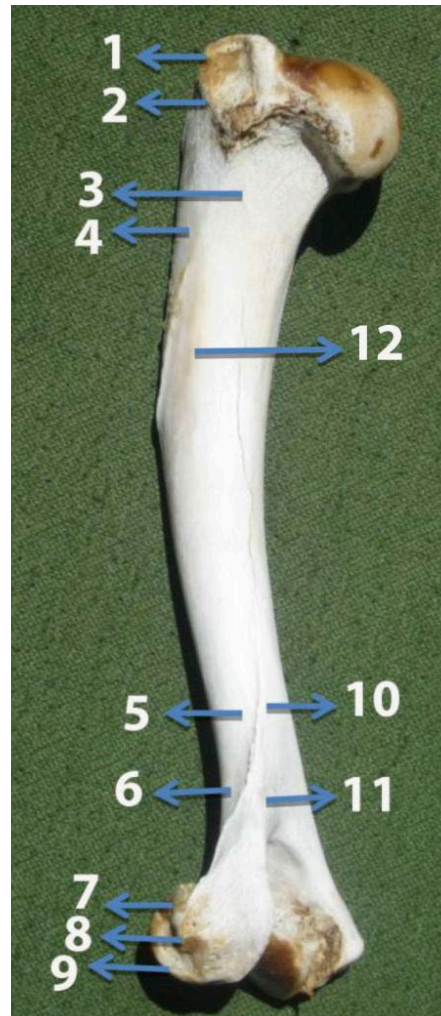
Figure 3. Caudolateral view of humerus: 1) Insertion of infraspinatus, 2) Teres minor tubercle and insertion of teres minor, 3) Origin of brachialis, 4) Origin of lateral head of triceps, 5) Origin of extensor carpi radialis, 6) Origin of extensor digitorum communis, 7) Origin of extensor digitorum lateralis, 8) Origin of extensor carpi ulnaris, 9) Origin of supinator, 10) Origin of brachioradialis, 11) Origin of anconeus, 12) Musculospiral groove.
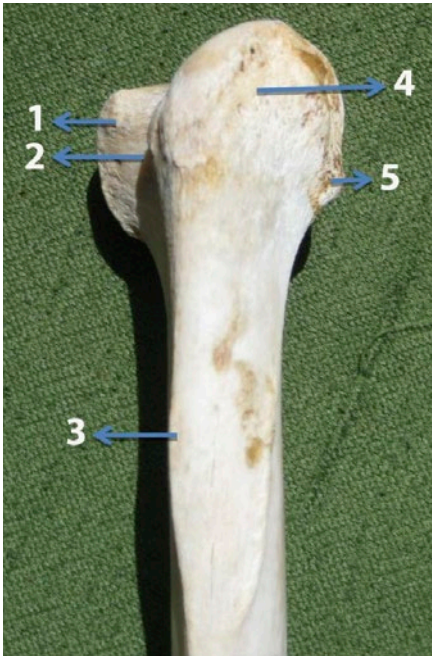
Figure 4. Cranial view of proximal half of humerus: 1) Lesser tubercle, 2) Intertuberal groove, 3) Deltoid tuberosity, 4) Greater tubercle, 5) Teres minor tuberosity.

Radius

The radius formed the elbow joint with the humerus above - therefore it possessed two articular surfaces separated by a groove - and a carpal joint with the proximal row of carpal bones below, where it presented three articular surfaces. The radius appeared as a transversely oval tube in cross section. The proximal extremity was expanded to form the radial head which was distinctly separated from the shaft by a marked radial column (Figs. 7, 8). The radial fovea capitis on the proximal surface of the head of the radius was shallow. On each side of the head, just below the margin of the articular surface, there was a tuberosity (Figs. 7, 8). The medial
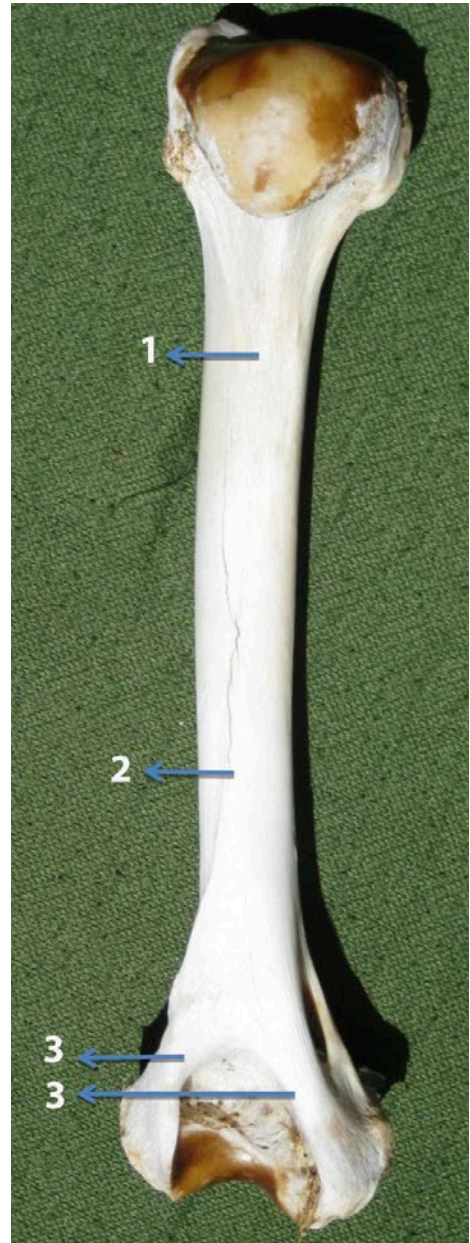
Figure 5. Caudal view of humerus: 1) Origin of accessory head of triceps, 2) Origin of brachioradialis, 3) Origin of anconeus.

Figure 6. Cranial and caudal view of the distal extremity of humerus: 1) Supracondyloid foramen, 2) Medial epicondyle, 3) Lateral epicondyle, 4) Lateral epicondyloid crest, 5) Radial fossa, 6) Olecranon fossa, 7) Origin of brachioradialis, 8) Origin of anconeus.

one was continuous with the radial tuberosity which lied dorsomedially (Fig. 8). The other one, which lied caudally on the head of the radius, provided for articulation with ulna (Fig. 8-1).

The long shaft was flattened craniocaudally. It presented four surfaces. The anterior surface was curved anterior-concave and smooth (Fig. 7). On this surface, in its distal part, this surface presented three grooves for the accommodation of the tendons of extensor muscles (Fig. 7). At the middle of the upper part of this surface there was a rough elevation, known as radial tuberosity (Figs. 7, 8). The posterior surface was concave and showed a non–articular eminence (Fig. 8). The lateral surface was rounded and smooth and the medial surface was smooth. The distal extremity was compressed craniocaudally to form the trochlea which articulated with the proximal row of carpal bones. Proximal to the articular surface, a transverse crest was found on the caudal surface of the radius (Fig. 8). There was a greater tuberosity to insert the tendon of brachioradialis muscle on the distal of lateral surface of this bone (Fig. 7, 8).

Ulna

At the proximal end of the ulna, the olecranon projected beyond the radius. Its free end was expanded to form the olecranon tuber. There was a proximodistal groove on the lateral surface of the olecranon (Fig. 9). There was also an incisure at its base, where it lied against the radius. Proximal to the articular surface the sharp-bordered anconeal process projected cranially (Fig. 11), while distally and on either side the lateral and medial coronoid processes also projected forwards (Figs. 9, 11). Between the two processes there was the trochlear notch which was articulated with the articular circumference of the radius (Fig. 9). There was an articular surface extended in lateromedial direction on the trochlear notch. Also a broad articular surface was under the trochlea notch (Figs. 9, 11). Distal to the trochlear notch the ulna was rough where it faced the radius.

Figure 7. Cranial surface of radius: 1) Insertion of supinator, 2) Insertion of brachioradialis, 3) Radial (medial) styloid process, 4,5,6) Medial, middle and lateral groove respectively, 7) Radial tuberosity. Notice the diaphysis curvature.
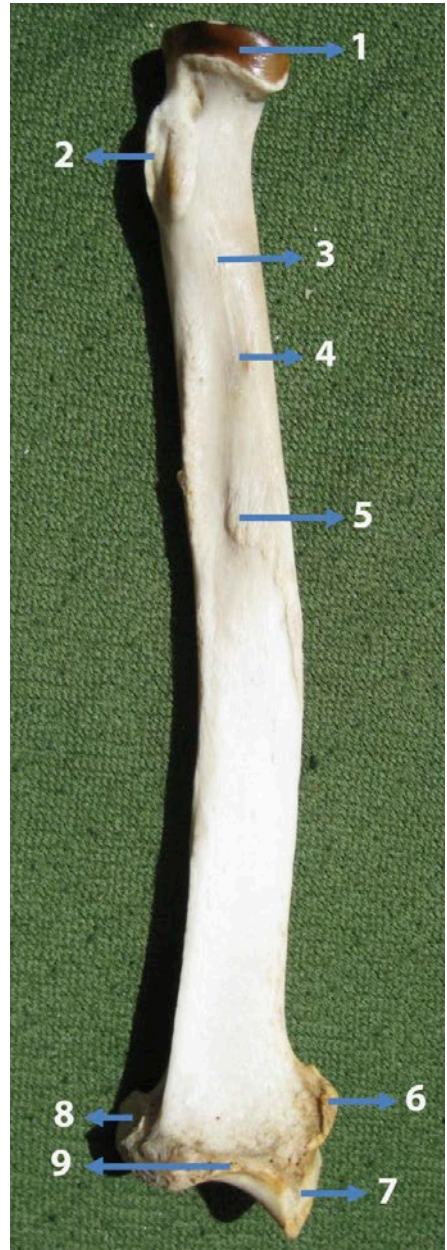
Figure 8. Caudal surface of radius: 1) Radial head, 2) Radial tuberosity, 3) Insertion of biceps brachialis, 4) Insertion of brachialis, 5) Origin of radial head of deep digital flexor tendon, 6) Insertion of brachioradialis, 7) Radial (medial) styloid process, 8) Ulnar notch, 9) Transverse crest.

Figure 9. Lateral surface of ulna: 1) Olecranon tuberosity and insertion of triceps, 2) Olecranon tuberosity and insertion of anconeus, 3) Trochlear notch, 4,5) Coronoid process, 6) Lateral styloid process.
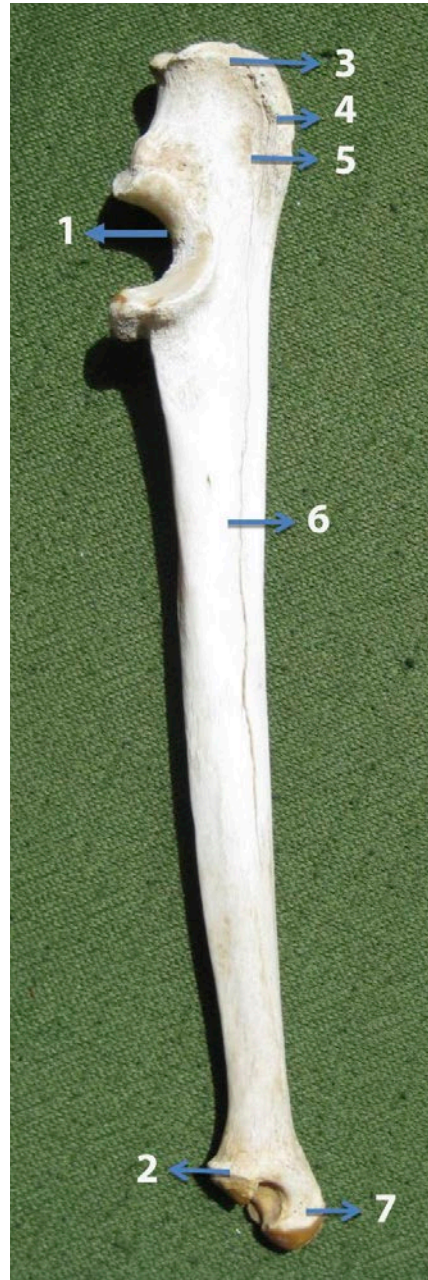
Figure 10. Medial surface of ulna: 1) Trochlear notch, 2) Radial notch, 3) Insertion of triceps, 4) Insertion of anconeus muscle, 5) Origin of ulnar head of flexor carpi ulnaris, 6) Ulnar head of deep digital flexor tendon, 7) Lateral styloid process.
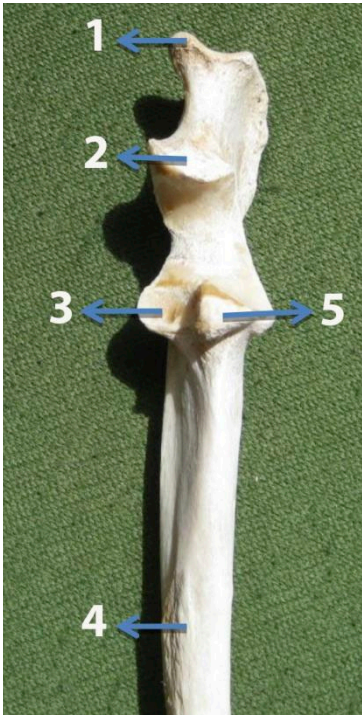
Figure 11. Cranial surface of the proximal half of ulna: 1) Olecranon tuberosity, 2) Anconeal process, 3,5) Coronoid process, 4) Insertion of pronator quadratus.

The shaft of the ulna was triangular in section and, like the radius, it was slightly convex cranially. The proximal half of the shaft in this bone was as thick as the distal one in caudal view. On the other hand, along the craniocaudal axis the upper part of the diaphysis was significantly longer than the distal part (Fig. 9, 10). There were two fossae on the lateral and medial surfaces of the shaft, the medial one was deeper than the other. Also, there was a broad non-articular eminence on the lateral surface of the shaft (Fig. 9).

The ulna was tapered distally. The olecranon tuber ended in three prominences. Two were cranial and with thin borders, while the third was caudal. The trochlear notch of the Asiatic cheetah was divided by a sagittal ridge into a larger lateral and a smaller medial surface. The medial coronoid process was broad, the lateral process was narrow and the anconeal process projected hook-like (Fig. 9, 11). The radial notch was concave and corresponded to the convex articular circumference of the radius (Fig. 10). The lateral styloid process projected distally and had a deeply convex articular surface for articulation with the carpal bones (Fig. 9, 10). Medially it had a convex articular circumference which joined with the radius.

As mentioned before, the shaft was roughly prismatic, so it had three surfaces and three borders. The anterior surface was articulated with the posterior lateral aspect of the radius (Fig. 11). At the upper part of the anterior surface there were two articular facets for articulation with the corresponding facets of radius (Fig. 11). The medial surface was smooth and concave. The proximal end was expanded and comprised one large olecranon process and a semilunar notch (Fig. 10). The olecranon process had two surfaces and two borders. The lateral surface was convex and the medial one was concave (Fig. 9, 10). The anterior border was limited by a semilunar notch and thereby formed a beak like projection, known as anconeal process (Fig. 11).

B) Osteometric analysis

The results are summarized in Table 1. Based on obtained data humerus was longer and thicker than radius.

Table 1. Measures of humerus, radius and ulna. Measures are given as mean ± standard error (cm), N = 5.

	GL	GLC	BP	BD	SD	DPA	SDO	BPC
Humerus	20.2±0.22	19.66±0.27	3.51±0.28	4.21±0.36	1.17±0.24	-	-	-
Radius	17.07±0.31	-	1.05±0.09	1.82±0.23	0.5±0.02	-	-	-
Ulna	21.31±0.2	-	-	-	-	2.46±0.18	2.06±0.32	1.99±0.04

GL: greatest length along the long axis of the bone, GLC: greatest length from caput (head) along the long axis, BP: greatest breadth of the proximal end, BD: greatest breadth of the distal end, SD: smallest breadth of the diaphysis, DPA: depth across processus anconaeus, SDO: smallest depth of the olecranon, BPC: greatest breadth across the coronoid process.

Discussion

Quadrupeds typically support a greater proportion of their body weight with their forelimbs during steady state locomotion (Alexander and Jayes, 1983; Witte et al., 2004) and, with increasing speed, peak GRFs have been shown to increase (Witte et al., 2004). When travelling at top speed cheetah's forelimbs are therefore likely to experience very high peak forces, and must be particularly adapt to resist large GRF joint torques. A long moment arm would increase the leverage that the muscle exerts at the joint (enabling a bigger joint torque for a given change in muscle length), maximizing the joint torque that can be achieved. Contrary to this, the forelimbs of quadrupeds are often thought of as springy struts (Blickhan, 1989; Blickhan and Full, 1993), where the GRF vector is aligned through the point of rotation of the forelimb on the body, resulting in small GRF joint torques, particularly at the shoulder (Carrier et al., 2008).

Maintaining a longer stance time will help to limit the peak vertical forces that the cheetah's limb experiences whilst maintaining the impulse required to support its own body weight when travelling at a given speed. Therefore, if peak force is a limit to an animal's maximum speed, this may be a way for cheetah to maintain higher duty factors when travelling at low speeds, enabling it to attain higher maximal speeds. This will be of great importance in the forelimb, as the forelimbs tend to support a larger proportion of an animal's body weight during steady state locomotion (Witte et al., 2004). According to results of Hudson et al. (2011) the cheetah's humerus and radius are heavier than the greyhound's, which will be essential for maintaining bone strength and safety factors (Alexander, 1993; Sorkin, 2008), but this will increase the inertia of the limb. Increased inertia would result in a longer swing time or more muscular work to accelerate and decelerate the limb through swing (Hudson et al., 2011).

As mentioned in a previous study (Hudson et al., 2011) that is in agreement with our observations, the olecranon tuberosity in the cheetah is proportionally greater than that in the cat. Triceps is one of the muscles which insert to it. Cheetah's musculoskeletal system must modulate and control the high speed maneuvering of its hunting style (Hudson et al., 2011). To prevent excessive joint torque, damage or instability at the elbow, the long head of triceps functions to extend the joint during stance (English, 1978). These hypotheses may justify the large olecranon tuberosity in the Asiatic cheetah.

According to a study in the cheetah, the forelimb musculature comprises 15.1 ± 1.2% of its total body mass, substantially less than its hindlimb which comprises 19.8 ± 2.2% of total body mass (Hudson et al., 2011). Pasi and Carrier (2003) suggested that the forelimbs of highly specialized runners would contain less muscle mass than the hindlimbs, as the forelimbs play a greater role in deceleration compared with the hindlimbs, which accelerate the centre of mass. This is because during deceleration muscles contract eccentrically (high force output), actively stretching to absorb energy, compared with the concentric (low force output) contractions used during accelerations, and therefore the forelimbs can contain muscles with smaller physiological cross-sectional areas to achieve the same force output (Hudson et al., 2011). It seems that the column of forelimb in the Asiatic cheetah is designed to reach this target because of its relatively extended length and small diameter. Increasing in length of a bone leads to increase the mass of the muscles around it. According to some studies many of the cheetah's proximal intrinsic limb muscles are larger in mass than those in the greyhound (Hudson et al., 2011). They also have longer maximum moment arms in the cheetah when compared with felids, enabling to produce larger joint torques but reducing the capacity to produce high joint rotational velocities (Hudson et al., 2011; Williams et al., 2008). We hypothesize the large muscle mass and long bones leads to stronger levers to run, jump and hunt in this animal.

Carrier et al. (2006) suggested that the serratus ventralis muscle functions for weight support while Hudson et al. (2011) suggested that the activity of this muscle causes the scapula translation and rotation that is observed in domestic cats. It was suggested that when both vertical and horizontal movements of the scapula during locomotion (Hildebrand, 1961, Hudson et al. 2011) combine with movements of long bones of the column of the forelimb in the cheetah they will enable longer strides, contact lengths and a more vertical limb at the extremes of stance, potentially aiding faster top speeds. It is required to withstand a larger joint torque, especially in the shoulder joint. The ability of some forelimb muscles to create larger joint torques in the cheetah will aid in this function, which will be of great importance at high speeds, when peak limb forces are likely to be higher (Witte et al., 2006, 2004). The high speed maneuvering that is characteristic of cheetah's hunting style also results in high limb forces (Hudson et al., 2011). Furthermore, the deep and extensive articular surface increases resistance to these forces.

According to some studies many of the cheetah's proximal intrinsic limb muscles are larger in mass than them in the greyhound (Hudson et al., 2011). They also have longer maximum moment arms in the cheetah when compared with felids, enabling to produce larger joint torques but reducing the capacity to produce high joint rotational velocities (Hudson et al., 2011; Williams et al., 2008). We hypothesize the large muscle mass and long bones leads to stronger levers to run, jump and hunt in this animal.

The cheetah possesses an additional muscle – the brachioradialis. It functions to supinate the paw, which is of crucial importance to the cheetah (Gorman and Londei, 2000; Russell and Bryant, 2001) and Asiatic cheetah for prey capture (Hudson et al., 2011). As shown in figures 3, 5, 7 and 8, the origin and insertion of this muscle is defined on both humerus and radius in Asiatic cheetah. It seems that the skeletal column in Asiatic cheetah is adapted to this muscle and its function. So the extensive articular surfaces, long shafts and small diameter of these two bones and the correlat-

ed decrease in muscle mass results in increasing the flexibility of forelimb according to Asiatic cheetah´s characteristics such as running, hunting and jumping.

According to origin and insertion of brachioradialis muscle (Fig. 3,5,6,7,8), cheetah can throw its forelimb to the front and stay in this position during jumping in high speeds. This action occurs due to movement of the shoulder joint and the activity of some extrinsic muscles of forelimb. As mentioned before, the length of the bones in this region acts as a lever and helps to long jumping. Tubers that relate with origin and insertion of brachioradialis muscle in cheetah are bigger than in the cat. It means that this muscle is more powerful in the cheetah than that in the cat and can exert a bigger force to move the forelimb and decrease swing time. Also this muscle is a supinator muscle and because of its long fascicles is apt for rapid joint rotation. According to Gorman and Londei (2000) and Russell and Bryant (2001) this muscle can cause at high velocity to rotate the joint through large angles. For this purpose this animal needs the extensive articular surfaces in the elbow, that we could show. Despite this, previous work on cheetah's elbow has highlighted a reduced ability for supination when compared with other felids, with a conformation much like canides and other runner carnivores (Andersson, 2004), contradicting muscular anatomy (Hudson et al., 2011).

There are some comparative studies between musculoskeletal anatomy of the cheetah forelimb and racing greyhound (Usherwood and Wilson, 2005; Williams et al. 2008). Williams et al. (2008) suggested that the large mass of muscle they observed in greyhound forelimbs may be used in propulsion or for bodyweight support. The fibers of forelimb muscles were considerably longer in the cheetah, which indicates a greater capacity for modulation of the muscle force–length relationship, and hence limb stiffness and mechanical work during stance. As a result of previous study, when scaled to body mass, the cheetah's radius (P<0.01) and humerus (P<0.05) were found to be significantly longer than those of the greyhound. The length of the bones acts as a lever and provides a bigger joint torque. Our obtained data for both humerus and radius were similar to those given for cheetah.

According to Alrtib et al. (2013) when the limb is landing either straight or towards the lateral side, the lateral condyle receives much more load per unit area than the medial condyle in a short period of time during the start of the weight bearing phase before the long lateral sides of the bones displace the load towards the medial condyle. Additionally, a significant difference in depth and width between the medial and lateral condyle was found in the current study, where the depth and width of the lateral condylee were significantly lower than those of the medial condyle. These results indicate that there is a difference in the surface area that receives the load in the contact phase. Eckstein et al. (2009) suggested that the increase in the surface area of bone can distribute the load over a wider area and consequently lead to a decrease in the mechanical stress on the surface. A similar condition occurs in racing horses. In racing horses, taking the relative size of the condyles into account, the high predisposition to lateral condylar fractures (Zekas et al., 1999; Radtke et al., 2003) might be related to a high load that may occur on the lateral condyle in the short period of time during the start of the weight-bearing phase. It also suggests that in the horses the thicker cartilage layer on the lateral condyle (Muir et al., 2008) may simply be a result of compensation associated with the relatively smaller surface area of the condyle itself. It seems likely that torsion of the bone can occur in some cir-

cumstances during the weight-bearing phase and this would be likely to make the long lateral side more susceptible to fracture (Alrtib et al., 2013). According to this hypothesis, it may be that the lateral condyle of humerus in cheetah has a high risk of fractures.

Acknowledgments

References

Alexander R.M.N. (1985) The maximum forces exerted by animals. J. Exp. Biol. 26: 231–238.

Alexander R.M.N. (1993) Optimization of structure and movement of the legs of animals. J. Biomech. 26 (Suppl. 1): 1–6.

Alexander R.M.N., Jayes A.S. (1983) A dynamic similarity hypothesis for the gaits of quadrupedal mammals. J. Zool. 201: 135–152.

Alrtib AM, Philip CJ, Abdunnabi AH, Davies HMS (2013) Morphometrical study of bony elements of the forelimb fetlock joints in horses. Anat. Histol. Embryol. 42: 9–20.

Andersson K.I. (2004) Elbow-joint morphology as a guide to forearm function and foraging behaviour in mammalian carnivores. Zool. J. Linn. Soc. 142: 91–104.

Blickhan R. (1989) The spring-mass model for running and hopping. J. Biomech. 22: 1217–1227.

Blickhan R., Full R.J. (1993) Similarity in multilegged locomotion: bouncing like a monopode. J. Comp. Physiol. A. 173: 509–517.

Carrier D.R., Deban S.M., Fischbein T. (2006) Locomotor function of the pectoral girdlemuscular 'sling' in trotting dogs. J. Exp. Biol. 209: 2224–2237.

Carrier D.R., Deban S.M., Fischbein T. (2008) Locomotor function of forelimb protractor and retractor muscles of dogs: evidence of strut-like behavior at the shoulder. J. Exp. Biol. 211:150-162.

Cavagna G.A., Franzetti P., Heglund N.C., Willems P.A. (1988) The determinants of the step frequency in running, trotting and hopping in man and other vertebrates. J. Physiol. 399: 81–92.

Day L.M., Jayne B.C. (2007) Interspecific scaling of the morphology and posture of the limbs during the locomotion of cats (Felidae). J. Exp. Biol. 210: 642–654.

Eckstein F., Hudelmaier M., Cahue S., Marshall M., Sharma L. (2009) Medial-to-lateral ratio of tibiofemoral subchondral bone area is adapted to alignment and mechanical load. Calcif. Tissue. Int. 84: 186–194.

English A.W. (1978) An electromyographic analysis of forelimb muscles during overground stepping in the cat. J. Exp. Biol. 76: 105–122.

Evans H.E., de Lahunta A. (2013) Miller´s Anatomy of the Dog. 4th edn. Philadelphia, W. B. Saunders Company. Pp. 177–196.

Farhadinia M.S. (2004) The last stronghold: cheetah in Iran. Cat News. 40: 11–14.

Getty R. (1975) The Anatomy of the Domestic Animals. Philadelphia, W. B. Saunders Company. Pp. 255–348.

Gonyea W., Ashworth R. (1975) The form and function of retractile claws in the felidae and other representative carnivorans. J. Morphol. 145: 229–238.

Gorman M.L., Londei T. (2000) The cheetah (Acinonyx jubatus) dewclaw: specialization overlooked. J. Zool. 251: 535–537

Heglund N.C., Taylor C.R. (1988) Speed, stride frequency and energy cost per stride: how do they change with body size and gait? J. Exp. Biol. 138: 301–318.

Hildebrand M. (1961) Further studies on locomotion of the cheetah. J. Mammol. 42: 84–91.

Hudson P.E., Corr S.A., Payne-Davis R.C., Clancy S.N., Lane E., Wilson A.M. (2011) Functional anatomy of the cheetah (Acinonyx jubatus) forelimb. J. Anat. 218: 375–385.

Hunter L., Hamman C. (2003) Cheetah. Cape Town (South Africa), Struik Publishers.

Keller T.S., Weisberger A.M., Ray J.L., Hasan S.S., Shiavi R.G., Spengler D.M. (1996) Relationship between vertical ground reaction force and speed during walking, slow jogging, and running. Clin. Biomech. 11: 253–225.

Lee D.V., Stakebake E.F., Walter R.M., Carrier D. (2004) Effects of mass distribution on the mechanics of level trotting in dogs. J. Exp. Biol. 207: 1715–1728.

Muir P., Peterson A.L., Sample S. J., Scollay M.C., Markel M.D., Kalscheur V.L. (2008) Exercise-induced metacarpophalangeal joint adaptation in the Thoroughbred racehorse. J. Anat. 213: 706–717.

Nickel R, Schummer A, Seiferle E (1973) The Anatomy of the Domestic Animals. 2nd edn. Berlin and Humburg, Verlag Paul Parey. Vol. 3: 77–99.

O'Brien S. J., Johnson W.E. (2007) The evolution of cats. Sci. Am. 297: 68–75.

Ozkan Z.E., Dynk G., Aydin A. (1997) Investigations on the comparative gross anatomy of scapula, clavicula, skeleton brachii and skeleton antebrachii in rabbits (Oryctolagus cuniculus), guinea pigs (Cavia porcellus) and rats (Rattus norvegicus). J Heal. Sci. 11: 171-175.

Pasi B.M., Carrier D.R. (2003) Functional trade-offs in the limb muscles of dogs selected for running vs. fighting. J. Evol. Biol. 16: 324–332.

Radtke C.L., Danova N.A., Scollay M.C., Santschi E. M., Markel M.D., Da Costa Gomez T., Muir P. (2003) Macroscopic changes in the distal ends of the third metacarpal and metatarsal bones of Thoroughbred racehorses with condylar fractures. Am. J. Vet. Res. 64: 1110–1116.

Russell A.P., Bryant H.N. (2001) Claw retraction and protraction in the Carnivora: the cheetah (Acinonyx jubatus) as an atypical felid. J. Zool. 254: 67–76.

Simon J.M.D. (1996) Measurements of a group of adult female Shetland sheep skeletons from a single flock: a baseline for zooarchaeologists. J. Archaeol. Sci. 23: 593–612.

Sorkin B. (2008) Limb bone stresses during fast locomotion in the African lion and its bovid prey. J. Zool. 276: 213–218.

Sunquist M., Sunquist F. (2002) Wild Cats of the World. Chicago, Univ. of Chicago Press.

Turner A., Anton M. (1997) The Big Cats and their Fossil Relatives: an Illustrated Guide to their Evolution and Natural History. New York, Columbia University Press.

Usherwood J.R., Wilson A.M. (2005) Biomechanics: no force limit on greyhound sprint speed. Nature 438: 753–754.

Usherwood J.R., Wilson A.M. (2006) Accounting for elite indoor 200 m sprint results. Biol. Lett. 2: 47–50.

Von den Driesch A. (1976) A Guide to the Measurement of Animal Bones from Archaeological Sites. Peabody museum, Harvard University. Pp. 74–101.

Weyand P.G., Sternlight D.B., Bellizzi M.J., Wright S. (2000) Faster top running speeds are achieved with greater ground forces not more rapid leg movements. J. Appl. Physiol. 89: 1991–1999.

Williams S.B., Wilson A.M., Daynes J., Peckham K., Payne R.C. (2008) Functional anatomy and muscle moment arms of the thoracic limb of an elite sprinting athlete: the racing greyhound (Canis familiaris). J. Anat. 213: 373–382.

Williams T.M., Dobson G.P., Mathieu-Costello O., Morsbach D., Worley M.B., Phillips J.A. (1997) Skeletal muscle histology and biochemistry of an elite sprinter, the African cheetah. J. Comp. Physiol. B. 167: 527–535.

Witte T.H., Hirst C.V., Wilson A.M. (2006) Effect of speed on stride parameters in racehorses at gallop in field conditions. J. Exp. Biol. 209: 4389–4397.

Witte T.H., Knill K., Wilson A.M. (2004) Determination of peak vertical ground reaction force from duty factor in the horse (Equus caballus). J. Exp. Biol. 207: 3639–3648.

Yilmaz S. (1998) Macro-anatomical investigation on the skeletons of porcupine (Hystrics cristita). Anat. Histol. Embryol. 27: 293–296.

Zekas L. J., Bramlage L. R., Embertson R.M., Hance S. R. (1999) Characterisation of the type and location of fractures of the third metacarpal/metatarsal condyles in 135 horses in central Kentucky (1986–1994). Eq. Vet. J. 31: 304–308.